

Controlled Release of Dexamethasone in PCL/Silk Fibroin/Ascorbic Acid Nanoparticles for the Initiation of Adipose Derived Stem Cells into Osteogenesis

Chinnasamy Gandhimathi¹, Neo Xuan Hao Edwin¹, Praveena Jayaraman¹, Jayarama Reddy Venugopal², Seeram Ramakrishna² and Srinivasan Dinesh Kumar^{1*}

¹Cellular and Molecular Epigenetics Lab, Lee Kong Chian School of Medicine, Nanyang Technological University, Singapore

²Center for Nanofibers and Nanotechnology, Nanoscience and Nanotechnology Initiative, National University of Singapore, Singapore

Abstract

Mimicking hybrid extracellular matrix is one of the major challenges in bone tissue engineering. Biocomposite micro/nanoparticle of polycaprolactone (PCL), silk fibroin (SF), ascorbic acid (AA) and dexamethasone (DM) were fabricated by the electrospaying methods in order to generate an improved osteogenic environment for the proliferation and differentiation of adipose derived stem cells (ADSCs) into osteogenesis. Fabricated electrospayed micro/nanoparticle was characterized for particle morphology, hydrophilicity, porosity and FTIR analysis for bone tissue regeneration. FESEM micrographs of the nanoparticles revealed porous, fibreless, uniform particles with particle diameter in the range of 720 ± 1.8 nm - 3.5 ± 4.2 μ m. The drug release profile indicates that the sustained release of dexamethasone up to 10 days and degradation of nanoparticles around 13-20% after 60 days. ADSCs were cultured on these nanoparticles and were induced to undergo osteogenic differentiation in the presence of AA/DM. The cells morphology, proliferation and interaction were analysed by CMFDA dye extraction method, MTS assay and FESEM analysis respectively. ADSCs differentiation into osteogenesis was confirmed using alkaline phosphatase activity and mineralisation by Alizarin Red staining. The significance of AA and DM biomolecules initiates particular biological functions for the proliferation of ADSCs and differentiation into osteogenic lineages. The obtained results proved that the biocomposite PCL/SF/AA/DM micro/nanoparticle stimulated osteogenic differentiation and mineralisation of ADSCs for bone tissue regeneration.

Keywords: Polycaprolactone; Silk fibroin; Dexamethasone release; Bone tissue engineering; Mineralization.

Introduction

Bone fracture and bone injury are serious health problem in the world, every year more than 2 million bone graft techniques are done in the United States [1,2]. Tissue engineering might offer a potential approach for bone repair [3,4]. For bone tissue engineering, scaffolds must have adequate mechanical strength similar to natural bone and be considered to support the adhesion, proliferation and differentiation of osteogenic precursor cells [5]. Biomaterials are mostly applied in the field of tissue engineering and have been considerably developed in recent years [5]. Among nanomaterials, nanoparticles have been supporting to develop scaffolds for biomedical engineering. Nanoparticles have potential properties, including size, shape, biocompatibility and selectivity in regenerative medicine. In addition, nanoparticles interact particularly with bone cells and tissues, depending on their composition, size, shape and surface properties. Meticulous analyses of nanoparticle effects on cellular functions have been made to select most appropriate candidates for supporting bone tissue regeneration [6]. Recently, electrospay (ES) method has expected great attention in the polymeric micro/nanoparticle production for tissue engineering [7,8]. In electrospay method, a Taylor cone is formed on the tip of spray nozzle and electrostatic potency induced by high voltage application can atomize various liquids into fine droplets [8-10]. Solvent evaporates during the spray of the droplets towards a grounded electrode [11]. The outstanding features of ES method are rapid and high efficiency, i.e. preparation of the solid nanoparticles in one step and entrapment of the drugs into nanoparticle without loss (100% entrapment efficiency) [11,12]. High entrapment efficacy is important for high drug loading capacity. Hence, ES method has potential to fabricate polymeric nanoparticles with high drug loading capacity in one step for the controlled release of drugs. Adipose tissue provides

an abundant source of multipotent stem cells which are capable of undergoing osteogenic differentiation [13,14]. Studies proved that adipose-derived stem cells (ADSCs) have similar immunophenotype, multilineage potential and transcriptome compared to bone marrow derived MSCs (BMSCs). Furthermore, ADSCs have many advantages like (i) they are abundant, (ii) more available and (iii) have lower donor morbidity, which in combination make ADSCs better substitute to BMSCs, particularly from a clinical perception where large cell numbers are required for regeneration, it appears that ADSCs are most suitable cell type for tissue engineering. Polycaprolactone (PCL) is a FDA approved polymer known for its biocompatibility, chemical stability, good mechanical properties, tissue-compatible nature and permeability [15]. Lack of surface functional groups and hydrophobic nature of PCL makes it difficult for cells to adhere and grow in tissue engineering. Silk proteins are potential materials as biomaterials owing to their slow biodegradability, biocompatibility, excellent mechanical property (tensile strength and Young's modulus) and appropriate structural morphology for tissue growth [16]. Stable, round, negatively charged and low toxic silk nanoparticles (150-170 nm) have been prepared from silk fibroin solutions of Bombyx mori and tropical tasar

***Corresponding author:** Srinivasan Dinesh Kumar, Cellular and Molecular Epigenetics Lab, Lee Kong Chian School of Medicine, Nanyang Technological University, Singapore, Tel: +65-65923055; E-mail: dineshkumar@ntu.edu.sg

Received March 11, 2015; Accepted April 24, 2015; Published April 30, 2015

Citation: Gandhimathi C, Edwin NXH, Jayaraman P, Venugopal JR, Ramakrishna S, et al. (2015) Controlled Release of Dexamethasone in PCL/Silk Fibroin/Ascorbic Acid Nanoparticles for the Initiation of Adipose Derived Stem Cells into Osteogenesis. J Drug Metab Toxicol 5: 177. doi:10.4172/2157-7609.1000177

Copyright: © 2015 Gandhimathi C, et al. This is an open-access article distributed under the terms of the Creative Commons Attribution License, which permits unrestricted use, distribution, and reproduction in any medium, provided the original author and source are credited.

silkworm *Antheraea mylitta* [17]. Silk fibroin and chitosan polymers were blended non-covalently to form nanoparticles (<100 nm) for local and sustained therapeutic curcumin delivery to cancer cells [18]. Furthermore, ascorbic acid (AA) is an important co-factor for the catalytic reaction of propyl hydroxylase enzymes that involves synthesis of extracellular matrix. Ascorbic acid enhances secretion of collagen matrix at many stages, including gene transcription, messenger RNA (mRNA) stabilization, translation and hydroxylation [19]. In addition to extracellular matrix (ECM) synthesis, AA regulates the differentiation of multi-potent precursor cells into bone cells by stimulation of integrin signalling and supporting cell matrix interaction [20]. The use of AA as an inducer of osteoblast differentiation would be an advantage in the treatment of bone-related diseases [21]. Dexamethasone (DM) is a synthetic steroidal anti-inflammatory drug which has been shown to induce osteogenic differentiation of MSCs in combination with ascorbate-2-phosphate and β -glycerophosphate [22]. DM is known to induce expression of osteogenic markers such as ALP, OCN, OPN, BMP, Type I Col, BSP and stimulate MSCs to form bone nodules [23,24]. In the present study, ADSCs cultured on PCL, PCL/SF, PCL/SF/AA and PCL/SF/AA/DM micro/nanoparticle to analyse the cell proliferation, osteogenic differentiation and mineralization for bone tissue regeneration.

Materials and Methods

Materials

Human adipose derived stem cells (ADSCs) were obtained from Lonza, (Allendale, NJ, USA). Dulbecco's modified eagle's medium/Nutrient Mixture F-12 (HAM), fetal bovine serum (FBS), antibiotics and trypsin-EDTA, CMFDA (5-chloromethyl-fluorescein diacetate), was procured from Invitrogen (Life Technologies, CA, USA). CellTiter 96[®] Aqueous one solution was obtained from Promega, (Madison, WI, USA). Polycaprolactone (Mw 80,000), Alizarin Red-S, cetylpyridinium chloride, ascorbic acid, dexamethasone and, 1,1,1,3,3,3-hexafluoro-2-propanol (HFIP) were purchased from Sigma-Aldrich, Singapore. Silk fibroin procured from Zhang Peng International trading Ltd, Singapore.

Electrospray nanoparticles

PCL 10% (w/v), PCL/SF 80:20 (10%), PCL/SF/AA 75:20:5 (10%) and PCL/SF/AA/DM 70:20:5:5 (10%) solution was prepared in HFIP. All the polymeric composite solutions were stirred magnetically overnight at room temperature to ensure homogeneity. Then load the solution onto a 5 ml syringe which is attached to a 25G needle with a syringe pump (KD 100 Scientific Inc., Holliston, MA, USA) with a constant flow rate of 1ml/hr. The voltage of the electric field was set at 16-17 kV (Florida, USA). During the electrospraying process, we collect the particles with an aluminum foil wrapped collector plate, located at a distance of 14-16 cm from the needle. The collected samples were then stored in vacuum conditions for nanoparticle characterization and cell cultures studies for bone tissue engineering.

Characterization of nanoparticles

The morphology of particles were analysed with a field emission scanning electron microscope (FESEM, FEI-QUANTA 200F) at an accelerating voltage of 10 kV, after sputter coating with platinum (JEOL JFC-1200 fine coater). The average diameter of the particle was determined with ImageJ software (Image Java, National Institutes of Health, USA). The hydrophilicity/hydrophobicity of the particles was determined by the contact angle of sessile drop water with VCA optima surface analysis system (AST Products, Billerica, MA, USA). Porosity and pore size was determined by porosimetry. Functional

groups present in the particle was determined using Fourier transform infrared (FTIR) spectroscopic analysis on Avatar 380 (Thermo Nicolet, Waltham, MA USA) over a range of 400-4000 cm^{-1} at a resolution of 8 cm^{-1} .

Degradation and drug release

50 mg of particle samples were placed in 15 ml of PBS solution (pH 7.4) in an incubator at 37°C for fixed periods of time. Every 3 days once replaced the buffer solution from the samples. The degraded nanoparticles were rinsed carefully with distilled water and then air dried in vacuum, finally weighed the nanoparticles. Percentage weight loss was calculated from the dried weight before and after degradation using the following formula.

$$\text{Weight loss\%} = \frac{W_0 - W_d}{W_0} \times 100(\%)$$

Where W_0 is the original weight before degradation and W_d is the dry weight after degradation. The morphological changes of sample before and after degradation were analysed with FESEM at an accelerated voltage of 10 kV.

Dexamethasone (10 mg) was weighed and transferred to a 10 ml flask containing 10 ml of 0.1N HCl. Then 0.1 ml of this solution is transferred to another 10 ml flask to obtain solution of 10 $\mu\text{g/ml}$. The absorbance was taken on double beam UV spectrophotometer using λ_{max} at 243 nm. The absorbance values were plotted against concentration ($\mu\text{g/ml}$) to obtain the standard calibration curve. 10 mg of DM dissolved in methanol and made up the volume with more of methanol to make the standard stock solution of 1000 $\mu\text{g/ml}$. The aliquots (0.1, 0.2, and 0.3 up to 1.0 ml) of stock solution (1000 $\mu\text{g/ml}$) were transferred into 10 ml volumetric flask and volume was made up to 10 ml with PBS 7.4 pH to prepare concentration ranging from 10-50 $\mu\text{g/ml}$. The absorbance of these solutions was determined at 243 nm using UV spectrophotometer.

The DM release profile from DM-loaded PCL/SF/AA particles was studied in PBS, the composite micro/nanoparticle samples (50 mg) were placed in a centrifuge tube, followed by adding 10 ml PBS as the release medium. Then, the centrifuge tube was kept in incubator at 37°C for further study. At particular time intervals, aliquots of samples (1 ml) were taken from the release medium at particular time intervals and that quantity was substituted with 5 ml PBS solution (37°C, pH 7.4). Then, the amount of DM released at different time points upto 7 days was analysed using UV-visible spectrophotometer at 420 nm. With the support of the calibration curve of DM measured in the similar condition, DM release percentage was determined and plotted as the curve versus time according to the equation:

$$\text{Release (\%)} = \frac{\text{Released DM}}{\text{Total loaded DM}} \times 100 (\%)$$

In vitro cell culture

Human adipose derived stem cells (ADSCs) were obtained from Lonza, (Allendale, NJ, USA) cultured in DMEM/F12 media (1:1) supplemented with 10% FBS and 1% antibiotic solution (Sigma-Aldrich, Singapore) in a 75 cm^2 cell culture flask. Cells were incubated at 37°C in a humidified atmosphere containing 5% CO_2 for 6 days and changed the medium once in every 2 days. The electrospray nanoparticles collected on coverslips were inserted into the 24-well plate, anchored with a stainless steel ring. UV light was first used to sterilize the nanoparticles for 3 hours, followed by sterilization with 70% ethanol for 30 minutes. The samples were washed three times with phosphate buffer saline (PBS) to eliminate the residual solvents and then soaked in DMEM overnight before cell seeding. Cultured ADSCs were trypsinized by

adding 0.25% trypsin containing 0.1% EDTA. Trypsinized cells were centrifuged, calculated by trypan blue assay using hemocytometer and seeded on the biocomposite particles at a density of 1.0×10^4 cells/well and left in incubator for facilitating the cell growth and tissue culture polystyrene (TCP) used as a control.

Cell morphology

The cell morphology was analysed using FESEM (Hitachi S4300, FESEM). After 15 days of seeding cells on the particles, the media was removed from culture wells and the cells and nanoparticles were rinsed with PBS and fixed in 3% glutaraldehyde for 3 h. Subsequently, the nanoparticles were again washed with DI water and then dehydrated with increasing concentrations of ethanol (50%, 70%, 90% and 100% v/v) for 10 min. Then the samples were dried with hexamethyldisilazane (HMDS, sigma) overnight in fume hood. The samples were coated with platinum and the cell morphology was analyzed using FESEM at an accelerating voltage of 10 kV. In addition, 5-Chloromethylfluorescein Diacetate (CMFDA) fluorescent dye is used to observe the morphology of the live cells. The CMFDA composite is taken up by live cells and transits to cell-impairment and brightly fluorescent state within 2 h. Addition of CMFDA to the medium which permeates the cell membrane and is acted upon by cytosolic esterase resulting in the formation of a CMFDA derivative which is brightly fluorescent. It is subsequently simplified by glutathione S-transferase, and the CMFDA compound conjugates to intracellular thiols and changes to a cell-impermeant state.

Cell proliferation

The cell proliferation was determined using the colorimetric MTS assay (cell titer 96 Aqueous one solution Promega, Madison, WI, USA). The principle of this assay is that the reduction of yellow tetrazolium salt [3-(4,5-dimethylthiazol-2-yl)-5-(3-carboxymethoxyphenyl)-2-(4-sulfophenyl)-2H-tetrazolium in MTS to form purple formazan crystals by dehydrogenase enzymes secreted by mitochondria of metabolically active cells. The formazan dye shows the absorbance at 490 nm and the quantity of formazan crystals produced is directly proportional to the number of live cells. Prior to this assay, samples were rinsed with PBS to remove unattached cells followed by incubation with 20% MTS reagent in serum free DMEM/F12 medium for 3 hr. Thereafter aliquots were pipetted into 96 well plate and the samples were read in a spectrophotometric plate reader (FLUOstar OPTIMA, BMG Lab Technologies, Germany).

Alkaline phosphatase activity

Alkaline phosphatase activity (ALP) was determined by using alkaline phosphate yellow liquid substrate system for ELISA (Sigma Life Sciences, USA). In this reaction, ALP catalyzes the hydrolysis of colourless organic phosphate ester substrate, p-nitrophenyl phosphate (pNPP) to a yellow product, p-nitrophenol and phosphate. The micro/nanoparticles seeded with ADSCs were rinsed gently with PBS and added 400 μ l pNPP and then incubated 30 min until the colour of solution turns yellow. The reaction was then stopped by adding 200 μ l of 2N NaOH solution following which the yellow colour product was aliquot in 96-well plate and read in spectrophotometric plate reader at 405 nm.

Mineralization of osteogenic cells

Alizarin red-S (ARS) is dye that binds selectively to calcium salts is used to determine and quantify the mineralization of differentiated osteoblast cells. Particles with cells were washed twice with PBS and

fixed in 70% ice-cold ethanol for 1 h. These constructs were washed twice with DI H₂O and stained with ARS (40 mM) for 20 min at room temperature. After several washes with DI water observed under optical microscope and then the stain was eluted with use of 10% cetylpyridinium chloride for 1 h. The dye was collected and absorbance read at 540 nm in a spectrophotometer (Thermo Spectronics, Waltham, MA, USA).

Statistical analysis

All quantitative results were obtained from triplicate samples. Data were expressed as the mean \pm standard deviation (SD). Statistical analysis was carried out using unpaired Student's t-test. A value of $p \leq 0.05$ was considered to be statistically significant.

Results and Discussion

Characterization of nanoparticles

Nano/microparticles have huge potential properties such as size, shape, biocompatibility, high porosity and increased surface area in tissue engineering applications. The FESEM micrographs revealed spherical shape, porous and fibreless particles shown in Figure 1. The diameter of the particles obtained around 720 ± 1.8 nm to 3.5 ± 4.2 μ m. Nanoparticles were further characterised by water contact angle

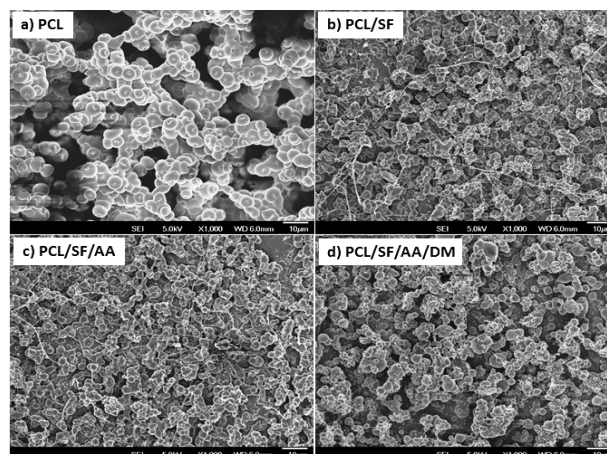


Figure 1: FESEM images of the electro sprayed micro/nanoparticles a) PCL b) PCL/SF, c) PCL /SF/AA and d) PCL /SF/AA/DM.

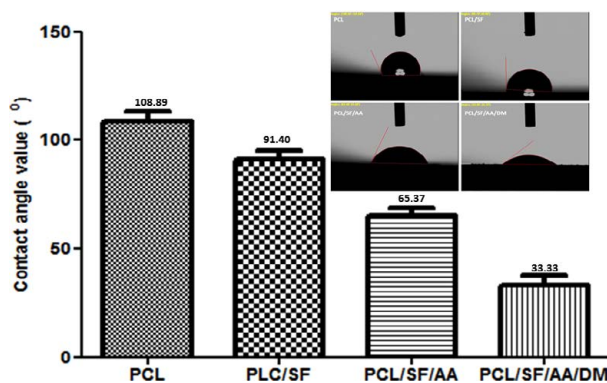


Figure 2: Contact angle value of PCL, PCL/SF, PCL/SF/AA and PCL/SF/AA/DM micro/nanoparticles.

analysis to confirm (Figure 2) the wettability of the particles, PCL nanoparticles are hydrophobic with contact angle of $108.89^\circ \pm 0.96$. The contact angles obtained for PCL/SF, PCL/SF/AA and PCL/SF/AA/DM were $91.40^\circ \pm 3.21$, $65.37^\circ \pm 2.38$ and $33.33^\circ \pm 2.43$ respectively (Table 1). The wettability of AA and water immersion property of SF has initiated hydrophilicity to the hydrophobic particles, thereby increasing their cell-adhesion property [25,26]. Pore size and porosity of the particles ranged between 1.5-9.5 μm and 42-57% respectively, indicating that the particles are highly porous in structure (Table 1). Pore size obtained for PCL/SF/AA/DM was greater than PCL/SF/AA which could be due to the difference in particle diameters that affects the arrangement between particles and then the pore size (Table 1) of the samples, conductivity of the solution provides greater charge capacity and stronger the widening forces, thus leading to decrease in particle diameter [27,28]. High porosity creates a significant feature of particles in order to permit for an efficient flow of nutrients and metabolic wastes [29]. The compound characteristics of functional groups on particles were analysed using FTIR spectroscopy as shown in Figure 3. The characteristic peak of C-O stretching in the crystalline phase, C=O ester stretching, asymmetric and symmetric C-H alkane stretching on PCL was noticed at $1,240\text{ cm}^{-1}$, $1,722\text{ cm}^{-1}$, $2,865\text{ cm}^{-1}$ and $2,949\text{ cm}^{-1}$ on the PCL nanoparticles. Similarly the specific peaks of amide I, II, and III of SF were also observed on the PCL/SF nanoparticles at $1,650\text{ cm}^{-1}$, $1,535\text{ cm}^{-1}$ and $1,250\text{ cm}^{-1}$. The characteristic peak of C=C and C-C ring stretching vibration of AA visualised on PCL/SF/AA particle at $1,660\text{ cm}^{-1}$ and 870 cm^{-1} . The characteristic peak of CH stretching vibration, carbonyl stretching of C-17 dihydroxyacetone side chain and carbonyl stretching vibration of C-3 observed in DM at $2,886\text{ cm}^{-1}$, $1,770\text{ cm}^{-1}$ and $1,660\text{ cm}^{-1}$ on PCL/SF/AA/DM nanoparticles.

Particles degradation and DM release

Biodegradable polymers attract more attention in tissue engineering

Particle construct	Particle diameter (μm)	Contact angle ($^\circ$)	Porosity (%)
PCL	3.5 ± 4.2	108.89 ± 0.96	57
PCL/SF	2.74 ± 5.4	91.40 ± 3.21	51
PCL/SF/AA	1.43 ± 2.2	65.37 ± 2.38	42
PCL/SF/AA/DM	0.72 ± 1.8	33.33 ± 2.43	48

Table 1: Characterization of nanofibrous particles

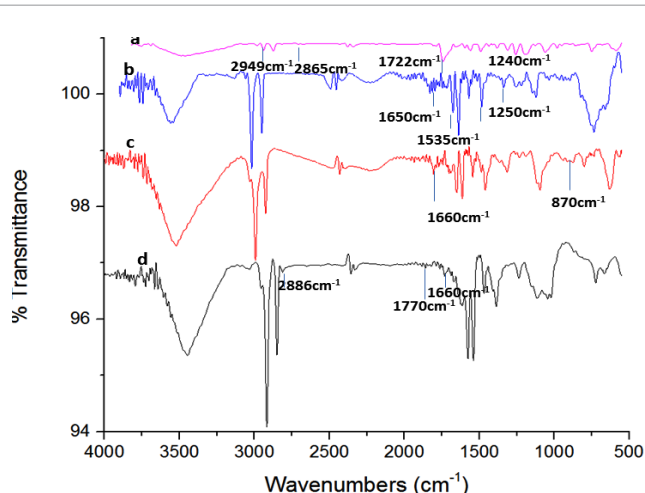


Figure 3: FT-IR spectroscopic analysis of PCL, PCL/SF, PCL/SF/AA and PCL/SF/AA/DM micro/nanoparticles.

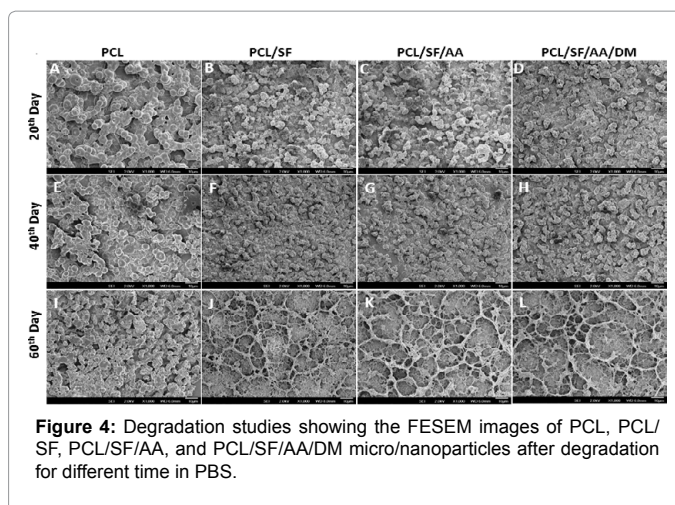


Figure 4: Degradation studies showing the FESEM images of PCL, PCL/SF, PCL/SF/AA, and PCL/SF/AA/DM micro/nanoparticles after degradation for different time in PBS.

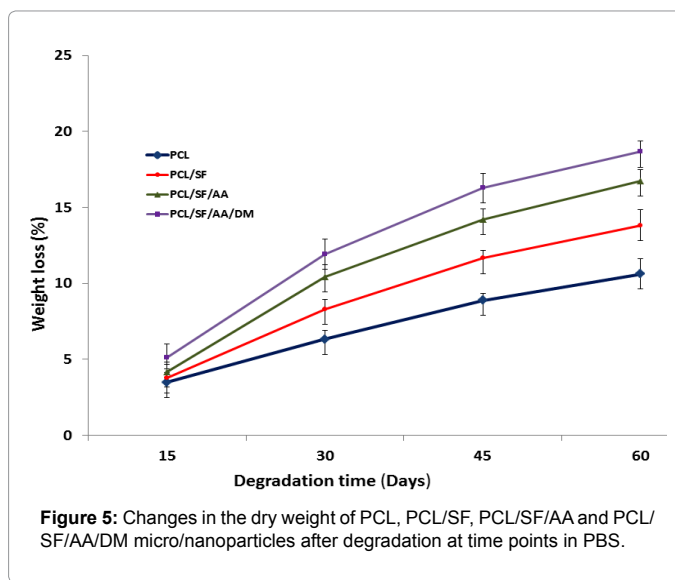


Figure 5: Changes in the dry weight of PCL, PCL/SF, PCL/SF/AA and PCL/SF/AA/DM micro/nanoparticles after degradation at time points in PBS.

because the high molecular weight chains would be hydrolysed into oligomers which are nontoxic to human body. Degradation of PCL occurs by hydroxylation and partition of high molecular weight chains, followed by varying to CO_2 and water in the atmosphere of water or body fluid with or without enzyme. The morphological changes of PCL, PCL/SF, PCL/SF/AA, and PCL/SF/AA/DM nanoparticles on day 20, 40 and 60 in PBS were showed in Figure 4. After 20 days of degradation, for the PCL/SF, PCL/SF/AA and PCL/SF/AA/DM particles, both particles and pore structures remained same and a little part of particles was chopped. After 40 and 60 days of degradation, the PCL/SF, PCL/SF/AA, and PCL/SF/AA/DM particle degrade and finally, decompose into powders. This was because at initial degradation, some low polymers hydrolysed and diffused from the particles, which resulted in more loose structure of the particles and made water molecules diffuse into the particles more easily. Increasing time, the long chains of polymer hydrolysed and ruptured, which made the particles break into pieces. The weight loss was started by the degradation process, the fact that soluble oligomeric sub-stances could be dissolved in the degradation medium from the surface of polymer by the hydrolysis of polymer chains. Figure 5 shows the weight variation of PCL, PCL/SF, PCL/SF/AA, and PCL/SF/AA/DM particles from 15 to 60 days. The weight loss

of PCL particles was 8.88% and 10.62% after degradation for 40-60 days and the degradation rate was much slower than PCL/SF samples. After days 40 and 60, with the addition of SF in PCL/SF, PCL/SF/AA, and PCL/SF/AA/DM, the degradation rate was increased and the weight loss of 11.65% and 13.22%, and 14.22% and 16.74%, and 16.3% and 18.65% respectively. The observed results indicated that the pure PCL particles had the slower degradation rate when compared to PCL/SF, PCL/SF/AA, and PCL/SF/AA/DM particles. The main reason is that the crystallization of pure PCL was higher than that of electrospun PCL/SF, PCL/SF/AA, and PCL/SF/AA/DM particles. The cumulative release of drug DM loaded samples shown in Figure 6. DM release profile shows the maximum absorbance at 243 nm and standard curve obtained around 50 µg/ml. The *in vitro* drug release is an important parameter for drug delivery, the release characteristics of DM from the micro/nanoparticles calculated by drug-eluting membranes of different composition, namely, 5%, and 10%. Experiments were performed in triplicates and the error bars indicates the standard deviation. Initial burst release was observed around 10-15% in the first 40 h. A gradual sustained release was observed between 50 and 150 h. The lower drug concentrations (0.05% and 0.08%), negligible release was detected by the end of tenth day. The maximum released percentage of DM of 5% and 10% w/w DM-loaded samples were about 52%, 69% at the end of tenth day. There was no further release of the drug and the curve saturation reached at 52%, 69% on tenth day of 5% and 10% w/w DM-loaded particles. The novelty of the observed results is the minimization of initial burst release and the stimulus of gradual release could be due to stabilization of drug within the composite structures. The early low burst release could be the result of trace drugs adsorbed on the particle surface.

Cell proliferation

Cell growth including proliferation suggests that the first stage of message between the interaction of cells and particles, which is essential for differentiation of stem cells [30,31]. MTS assay (Figure 7) showed significant increase ($p \leq 0.05$) for day 10 and 15 of cell culture in the proliferation of ADSCs on PCL/SF/AA/DM particles as compared to PCL. On day 10 observed the proliferation of cells was 78% for PCL/SF/AA/DM particles compared to PCL particles. The observed results indicate that the modification of particle by addition of SF may change the particles architecture results in the proliferation of cells. Further, DM may stimulate cell attachment, proliferation and ascorbic acid stimulates various cellular reactions in a variety of cells. Studies proved

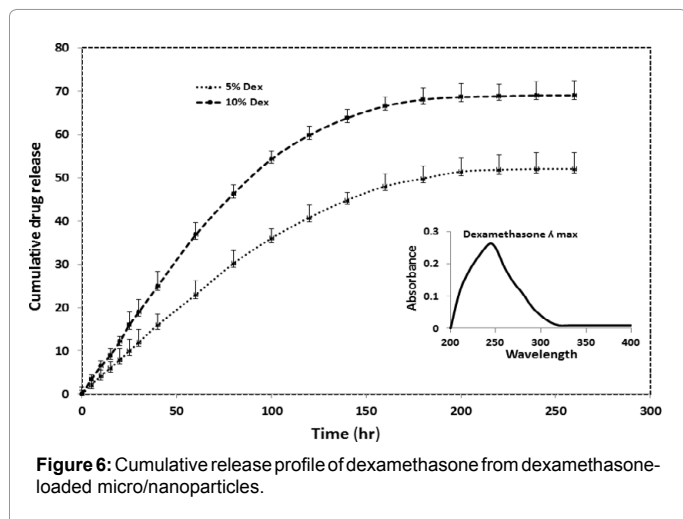


Figure 6: Cumulative release profile of dexamethasone from dexamethasone-loaded micro/nanoparticles.

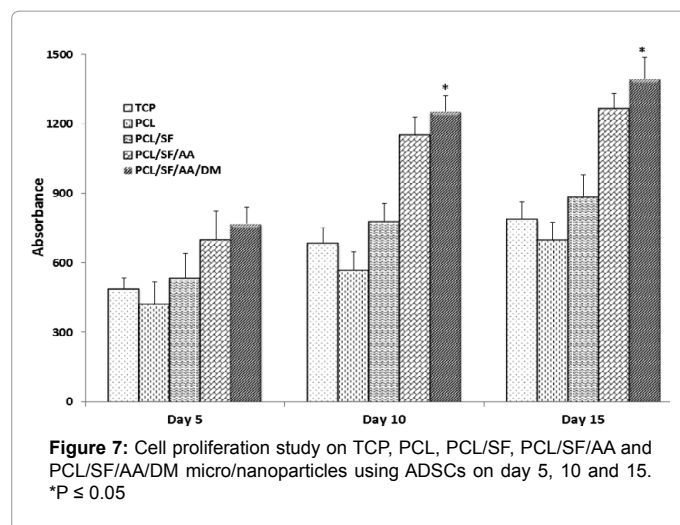


Figure 7: Cell proliferation study on TCP, PCL, PCL/SF, PCL/SF/AA and PCL/SF/AA/DM micro/nanoparticles using ADSCs on day 5, 10 and 15. * $P \leq 0.05$

that the proliferation and differentiation of ADSCs into skeletal tissues needs ascorbic acid as an important supplement in the complete medium [32]. Amino and hydroxyl groups found on the surface of PCL/SF, PCL/SF/AA and PCL/SF/AA/DM particles provide ligands for stimulating cell proliferation compared to particles lacking of any cell binding moieties like PCL alone.

Cell morphology

The interaction of cells with stratum forms the beginning of tissue organization. Therefore in order to examine the abilities of the particles in supporting arrangement of cells, we studied the biocomposite particles under field emission scanning electron microscope. Figure 8 shows the micrographs of ADSCs cultured on PCL, PCL/SF, PCL/SF/AA and PCL/SF/AA/DM particles (Day 15). It is evident from the figure that cells start to stabilize and align themselves in the PCL/SF, PCL/SF/AA and PLACL/SF/AA/DM particles. However, in the absence of SF, AA and DM the cellular organization is somewhat randomly distributed on TCP and the cells remain distributed and poorly aligned on PCL alone. The intercellular network on PCL/SF/AA/DM particles was also documented to be more to all other particles. The live cell image was noticed in CMFDA dye on day 15 in Figure 9. The cell-to-cell contact with elongated morphology was noticed on the PCL, PCL/SF particles. ADSCs leads to more cell density, osteogenic differentiation and cuboidal morphology observed on PCL/SF/AA/DM samples, as represented by arrows in figure 9(e).

Alkaline phosphatase activity

An active bone substitute must support better bone development containing organic and inorganic constituent of natural tissues. ALP is a main component of bone matrix vesicles because of its role in the development of apatite calcium phosphate and also main indicator of immature osteoblast activity [33]. The ALP activity (Figure 10) of ADSCs was significantly increased ($p \leq 0.05$) on PCL/SF/AA and PCL/SF/AA/DM samples compared to PCL and TCP on days 5 and 10. This is due to the presence of AA and DM which support mineralization process. The ALP activity was significantly ($P \leq 0.001$) increased in PCL/SF/AA/DM on day 10 and 15. This is because AA and DM known to encourage mineralization process of precursor cells as well as develops bone formation [34,35]. Higher levels of ALP activity were observed on PCL/SF/AA and PCL/SF/AA/DM particles on day 15; but there was no significant increase in the ALP activity from day 10 to 15 on PCL/SF/

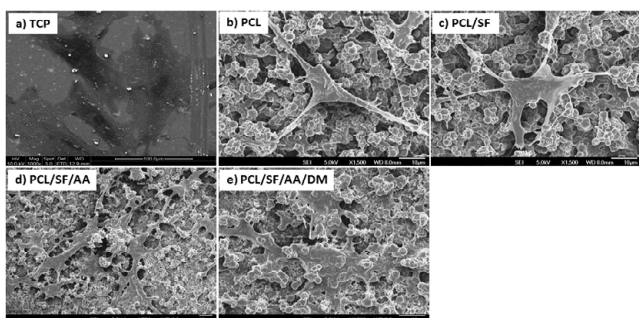


Figure 8: FESEM images showing the cell-biocomposite nanoparticles interaction on a) TCP, b) PCL, c) PCL/SF, d) PCL/SF/AA, e) PCL/SF/AA/DM micro/nanoparticles.

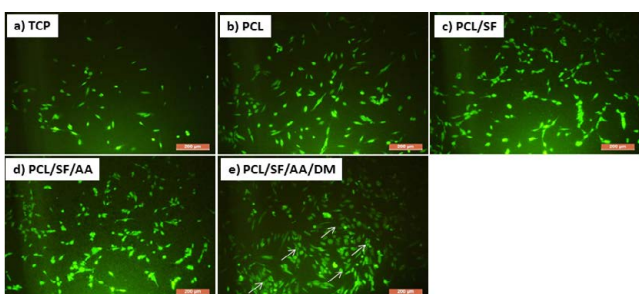


Figure 9: CMFDA dye extrusion image to analyse the cell morphology on a) TCP, b) PCL, c) PCL/SF, d) PCL/SF/AA, e) PCL/SF/AA/DM micro/nanoparticles at 10x magnifications. Arrows indicate the osteoblast-like morphology of the differentiated ADSCs.

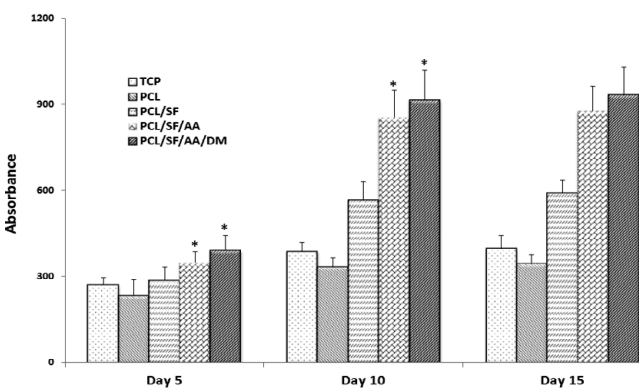


Figure 10: Alkaline phosphatase activity showing the osteogenic differentiation of ADSCs on TCP, PCL, PCL/SF, PCL/SF/AA and PCL/SF/AA/DM micro/nanoparticles on day 5, 10 and 15. *P<0.05.

AA and PCL/SF/AA/DM particles. This down-regulation of ALP at day 15 revealed that the cellular development changing onto further steps, such as differentiation and mineralization of ADSCs into osteogenesis.

Mineralization

Calcium mineralization was measured qualitatively as shown in Figure 11. The capacity to deposit more minerals is a sign of mature osteoblasts, which can be used to prove that the ADSCs seeded onto

particles have differentiated and reached the mineralization stage to deposit mineralized ECM. Compared to PCL, all other biocomposite particles had significant calcium phosphate deposition due to more differentiation observed in these particles in the presence of SF, AA and DM biomolecules. ADSCs cultured on PCL/SF/AA/DM particles (Figure 11e) observed faster interaction with more deposited minerals compared to all other particles. Quantitatively measured ARS staining revealed a significant increase of mineral deposition in PCL/SF/AA and PCL/SF/AA/DM ($P \leq 0.05$) particles compared to PCL on day 15 (Figure 12). ALP leads osteocalcin (OCN) in differentiation process; because ALP supports the production of ECM for the deposition before start of mineralization which is connected to OCN expression [36,37]. Mineralization of ADSCs is one of the main activities for bone tissue regeneration and obtained results suggest that the incorporation of DM upregulated the mineralization process, yielding more mineral deposition observed in Figure 9e for the differentiation of ADSCs into osteogenesis in bone tissue engineering.

Conclusions

The potential biocomposite components for effective tissue engineering include biodegradable particles with controlled release of bioactive molecules stimulating proliferation, differentiation and

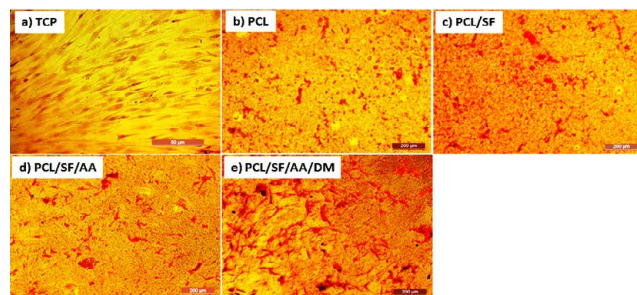


Figure 11: Optical microscope image showing the secretion of extracellular matrix by osteogenic differentiation of ADSCs using Alizarin red staining on day 15 (a-e) on TCP (a), PCL (b), PCL/SF (c), PCL/SF/AA (d) and PCL/SF/AA/DM (e) micro/nanoparticles at 10 X magnification.

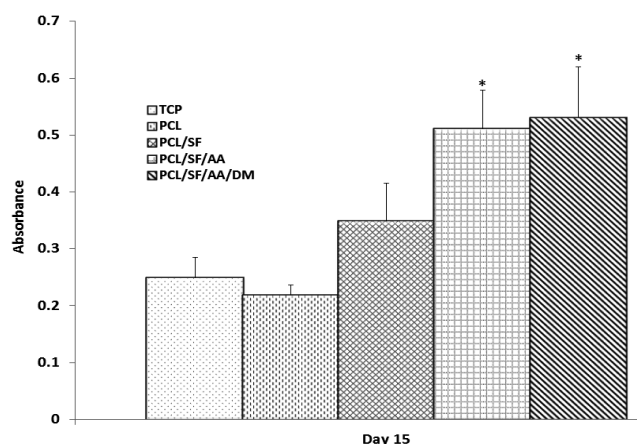


Figure 12: Quantification of mineral deposition in ADSCs differentiated into osteogenic lineage measured by the method of Alizarin Red-S staining on TCP, PCL, PCL/SF, PCL/SF/AA and PCL/SF/AA/DM micro/nanoparticles. *P < 0.05.

regeneration for subsequent implantation into the defective site of the host tissues. To facilitate the proliferation, high surface area and interconnected porous structures are important for the regeneration of the diseased tissues. Electrospay of DM loaded particles approach for bone tissue engineering applications by incorporating SF and AA with PCL particles to improve the favorable situation for ADSCs differentiation into osteogenesis and increased secretion of mineralization for bone formation. Therapeutic potentials of ADSCs cultured on PCL/SF/AA/DM composite particles hold great potential for cellular activities ranging from cell adhesion, migration, proliferation, differentiation, and mineralization for the treatment of bone defects in bone tissue engineering.

Acknowledgement

This work was supported by Ministry of Education Start-up grant (Srinivasan Dinesh Kumar), Lee Kong Chian School of Medicine, Nanyang Technological University, Singapore.

References

- Langer R, Vacanti JP (1993) Tissue engineering. *Science* 260: 920-926.
- Chen J, Chu B, Hsiao BS (2006) Mineralization of hydroxyapatite in electrospun nanofibrous poly(L-lactic acid) scaffolds. *J Biomed Mater Res A* 79: 307-317.
- Williams D (2004) Benefit and risk in tissue engineering. *Mater Today* 7: 24-9.
- Kneser U, Schaefer DJ, Polykandriotis E, Horch RE (2006) Tissue engineering of bone: the reconstructive surgeon's point of view. *J Cell Mol Med* 10: 7-19.
- Mitragotri S, Lahann J (2009) Physical approaches to biomaterial design. *Nat Mater* 8: 15-23.
- Tautzenberger A, Kovtun A, Ignatius A (2012) Nanoparticles and their potential for application in bone. *Int J Nanomedicine* 7: 4545-4557.
- Jung JH, Park SY, Lee JE, Nho CW, Lee BU, et al. (2011) Electrohydrodynamic Nano-spraying of Ethanolic Natural Plant Extracts. *J Aerosol Sci* 42: 725-736.
- Lee YH, Mei F, Bai MY, Zhao S, Chen DR (2010) Release profile characteristics of biodegradable-polymer-coated drug particles fabricated by dual-capillary electrospay. *J Control Release* 145: 58-65.
- Lee YH, Wu B, Zhuang WQ, Chen DR, Tang YJ (2011) Nanoparticles facilitate gene delivery to microorganisms via an electrospay process. *J Microbiol Methods* 84: 228-233.
- Zhang S, Kawakami K (2010) One-step preparation of chitosan solid nanoparticles by electrospay deposition. *Int J Pharm* 397: 211-217.
- Almeria B, Fahmy TM, Gomez A (2011) A multiplexed electrospay process for single-step synthesis of stabilized polymer particles for drug delivery. *J Control Release* 154: 203-210.
- Morozov VN (2010) Electrospay deposition of biomolecules. *AdvBiochem Eng Biotechnol* 119: 115-162.
- Zuk PA, Zhu M, Mizuno H, Huang J, Futrell JW, et al. (2001) Multilineage cells from human adipose tissue: implications for cell-based therapies. *Tissue Eng* 7: 211-228.
- Halvorsen YD, Franklin D, Bond AL, Hitt DC, Aughter C, et al. (2001) Extracellular matrix mineralization and osteoblast gene expression by human adipose tissue-derived stromal cells. *Tissue Eng* 7: 729-741.
- Dietzel JM, Kleinmeyer J, Harris D, Tan NCB (2001) The effect of processing variables on the morphology of electrospun nanofibers and textiles. *Polymer* 42: 261-272.
- Numata K, Kaplan DL (2010) Silk-based delivery systems of bioactive molecules. *Adv Drug Deliv Rev* 62: 1497-1508.
- Kundu J, Chung Y, Kim YH, Tae G, Kundu SC (2010) Silk fibroin nanoparticles for cellular uptake and control release. *Int J Pharm* 388: 242-250.
- Gupta V, Aseh A, Rios CN, Aggarwal BB, Mathur AB (2009) Fabrication and characterization of silk fibroin-derived curcumin nanoparticles for cancer therapy. *Int J Nanomedicine* 4: 115-122.
- Kadler KE, Baldock C, Bella J, Boot-Handford RP (2007) Collagens at a glance. *J Cell Sci* 120: 1955-1958.
- Franceschi RT (1992) The role of ascorbic acid in mesenchymal differentiation. *Nutr Rev* 50: 65-70.
- Wagner AE, Boesch-Saadatmandi C, Breckwoldt D, Schrader C, Schmelzer C, et al. (2011) Ascorbic acid partly antagonizes resveratrol mediated heme oxygenase-1 but not paraoxonase-1 induction in cultured hepatocytes-role of the redox-regulated transcription factor Nrf2. *BMC Complement Altern Med* 11:1.
- Jaiswal N, Haynesworth SE, Caplan AI, Bruder SP (1997) Osteogenic differentiation of purified, culture-expanded human mesenchymal stem cells in vitro. *J Cell Biochem* 64: 295-312.
- Peter SJ, Liang CR, Kim DJ, Widmer MS, Mikos AG (1998) Osteoblastic phenotype of rat marrow stromal cells cultured in the presence of dexamethasone, beta-glycerolphosphate, and L-ascorbic acid. *J Cell Biochem* 71: 55-62.
- Rickard DJ, Sullivan TA, Shenker BJ, Leboy PS, Kazhdan I (1994) Induction of rapid osteoblast differentiation in rat bone marrow stromal cell cultures by dexamethasone and BMP-2. *Dev Biol* 161: 218-228.
- Kay MI, Young RA, Posner AS (1964) Crystal Structure Of Hydroxyapatite. *Nature* 204: 1050-1052.
- Liu L, Liu J, Wang M, Min S, Cai Y, et al. (2008) Preparation and characterization of nano-hydroxyapatite/silk fibroin porous scaffolds. *J Biomater Sci Polym Ed* 19: 325-338.
- Reneker DH, Yarin AL (2008) Electrospinning jets and polymer nanofibers. *Polymer* 49: 2387-2425.
- Beachley V, Wen X (2009) Fabrication of Nanofiber Reinforced Protein Structures For Tissue Engineering. *Mater Sci Eng C Mater Biol Appl* 29: 2448-2453.
- Agrawal CM, Ray RB (2001) Biodegradable polymeric scaffolds for musculoskeletal tissue engineering. *J Biomed Mater Res* 55: 141-150.
- Gandhimathi C, Venugopal JR, Tham AY, Ramakrishna S, Kumar SD (2015) Biomimetic hybrid nanofibrous substrates for mesenchymal stem cells differentiation into osteogenic cells. *Mater Sci Eng C Mater Biol Appl* 49: 776-785.
- Beachley V, Wen X (2010) Polymer nanofibrous structures: Fabrication, biofunctionalization, and cell interactions. *Prog Polym Sci* 35: 868-892.
- Choi KM, Seo YK, Yoon HH, Song KY, Kwon SY, et al. (2008) Effect of ascorbic acid on bone marrow-derived mesenchymal stem cell proliferation and differentiation. *J Biosci Bioeng* 105: 586-594.
- Gandhimathi C, Venugopal J, Ravichandran R, Sundarajan S, Suganya S, et al. (2013) Mimicking nanofibrous hybrid bone substitute for mesenchymal stem cells differentiation into osteogenesis. *Macromol Biosci* 13: 696-706.
- Chuenjitkuntaworn B, Inrung W, Damrongsri D, Mekaapiruk K, Supaphol P, et al. (2010) Polycaprolactone/hydroxyapatite composite scaffolds: preparation, characterization, and in vitro and in vivo biological responses of human primary bone cells. *J Biomed Mater Res* 94: 241-251.
- Wang H, Li Y, Zuo Y, Li J, Ma S, et al. (2007) Biocompatibility and osteogenesis of biomimetic nano-hydroxyapatite/polyamide composite scaffolds for bone tissue engineering. *Biomaterials* 28: 3338-3348.
- Mizuno M, Kuboki Y (2001) Osteoblast-related gene expression of bone marrow cells during the osteoblastic differentiation induced by type I collagen. *J Biochem* 129: 133-138.
- Stein GS, Lian JB, van Wijnen AJ, Stein JL, Montecino M, et al. (2004) Runx2 control of organization, assembly and activity of the regulatory machinery for skeletal gene expression. *Oncogene* 23: 4315-4329.